

# Articles

## Polymerization of Diacetylene–Bis(toluenesulfonide) in a Porous Silica Matrix: Evidence of Polymer Chain Self-Orientation

Nicolas Errien,\* Jean-Yves Mevellec, Guy Louarn, and Gerard Froyer

Laboratoire de Physique des Matériaux et Nanostructures, UMR 6502, Institut des Matériaux Jean Rouxel, 44322 Nantes Cedex 03, France

Received January 12, 2005. Revised Manuscript Received March 4, 2005

We have tailored a new composite based on a porous silica matrix and poly(diacetylene–bis(toluenesulfonide)). The filling of the sample was characterized by energy-dispersive X-ray (EDX) and Raman scattering spectroscopies. Raman scattering, in the polarized mode, was used to check the orientation of the macromolecules in the polymer single crystal before using these data to probe the polymer chain orientation inside the nanocomposite. We have found that polymer chains are oriented along the pore axis with a fairly high conjugation length.

### Introduction

A large amount of work has been done on the template synthesis of conjugated polymers such as PEDOT, Ppy, and PANI<sup>1–4</sup> with the aim of investigating property changes between the bulk material and the template one.

On the other hand, extensive studies have been carried out on porous silicon because of its luminescence efficiency or for its sensing capability.<sup>5</sup> More recently, results on optical guiding in porous silicon were published, opening up a new potentiality for this material.<sup>6</sup>

In this paper, we describe a new nanocomposite based on a porous silica matrix (by oxidation of porous silicon) filled with a conjugated polymer, poly(diacetylene–bis(toluenesulfonide)) (PDA–TS), because this polymer exhibits very promising nonlinear properties<sup>7,8</sup> and is generally obtained with a high crystallinity. As silica is transparent in the infrared domain it is anticipated that this nanocomposite will fulfill the requirement to build near future components for all optical processing of optical signals in telecommunication networks.

### Experimental Section

Mesoporous silicon is obtained by electrochemical anodization of (100)-oriented highly bore-doped ( $\rho = 3\text{--}7\text{ m}\Omega\cdot\text{cm}$ ) silicon wafers in a fluorhydric acid solution, HF–distilled water–ethanol (2/2/1), as described elsewhere.<sup>9</sup> Planar waveguides can be obtained in the same way by using two different current densities. For example, in the first step a current density of  $50\text{ mA}\cdot\text{cm}^{-2}$  was used, leading to a 73% porosity in volume (guiding layer), and in the second step a current density of  $100\text{ mA}\cdot\text{cm}^{-2}$  allowed a second layer to be obtained with an 80% porosity (confinement layer). The as-obtained samples (either monolayers or bilayers) may then be oxidized under oxygen at 1023 K in a controlled atmosphere oven following a well-known procedure.

The monomer diacetylene–bis(toluenesulfonide) (DA–TS) was synthesized by the reaction of 2,4-hexadiyne-1,6-diol on *p*-toluenesulfonyl chloride<sup>10</sup> and was kept in the dark at low temperature to avoid polymerization.

Monomer crystals were obtained by slow evaporation of acetone from the monomer solution, and then were heated at 338 K for 24 h to complete the polymerization. Single crystals of  $10\text{ mm}^2$  with a thickness of 2 mm were produced, and X-ray diffraction data indicated a monoclinic unit cell ( $a = 14.52\text{ \AA}$ ,  $b = 4.90\text{ \AA}$ ,  $c = 15.02\text{ \AA}$ ,  $\alpha = \gamma = 90^\circ$ , and  $\beta = 118.3^\circ$ ), which is consistent with the literature.<sup>11</sup>

The filling of porous substrates was performed in three steps. The porous silica samples were first covered with a thin film of monomer powder and then pumped under vacuum to eliminate residual gas adsorbed within the porous matrix. Then, by saturating the atmosphere with acetone vapor (which is a very good solvent of DA–TS), monomer powder was dissolved and the saturated solution filled up the pores. After evaporation of acetone, the sample was heated for 48 h at 338 K to polymerize the monomer.

\* To whom correspondence should be addressed. E-mail: nicolas.errien@cnrs-imn.fr.

- (1) Duvail, J. L.; Rétho, P.; Garreau, S.; Louarn, G.; Godon, C.; Demoustier-Champagne, S. *Synth. Met.* **2002**, *131*, 123.
- (2) Skotheim, T. A.; Elsenbaumer, R. L.; Reynolds, J. R., Eds. *Handbook of Conducting Polymers*, 2nd ed.; Marcel Dekker: New York, 1998; see also references therein.
- (3) Delvaux, M.; Duchet, J.; Stavaux, P. Y.; Legras, R.; Demoustier-Champagne, S. *Synth. Met.* **2000**, *113*, 275.
- (4) Demoustier-Champagne, S.; Stavaux, P. Y. *Chem. Mater.* **1999**, *11*, 829.
- (5) Hérino, R. *Mater. Sci. Eng., B* **2000**, *70*.
- (6) Charrier, J.; Lupi, C.; Haji, L.; Boissier, C. *Mater. Sci. Semicond. Process.* **2000**, *3*, 357.
- (7) Luther-Davies, B.; Samoc, M. *Solid State Mater. Sci.* **1997**, *2*, 213.
- (8) Bjornholm, T.; Greve, D. R.; Geisler, T.; Petersen, J. C.; Jayaraman, M.; McCullough, R. D. *Synth. Met.* **1997**, *84*, 531.

- (9) Bisi, O.; Ossicini, S.; Pavesi, L. *Surf. Sci. Rep.* **2000**, *38*, 1 and references therein.
- (10) Wegner, G. *Makromol. Chem.* **1971**, *145*, 85.
- (11) Kobelt, Von D.; Paulus, E. F. *Acta Crystallogr., B* **1974**, *30*, 232.

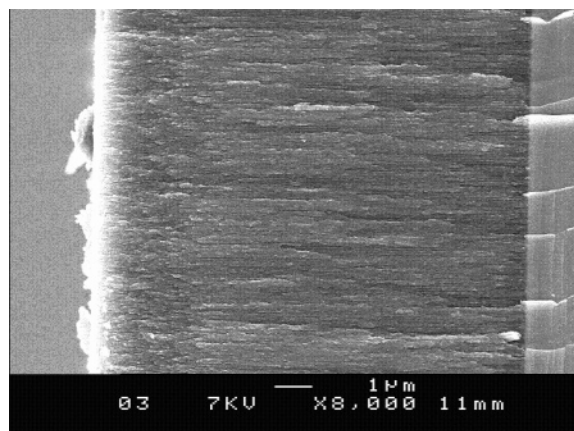


Figure 1. SEM side view of a porous silicon layer before thermal oxidation.

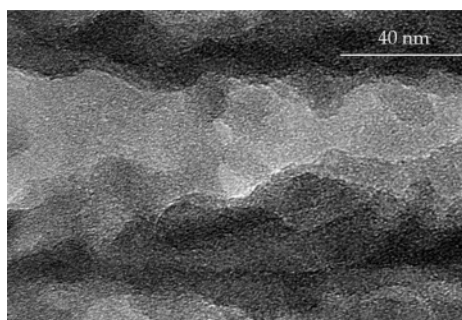


Figure 2. TEM side view of a pore in a porous silicon layer (pore walls are in black).

Optical absorption experiments were performed with a Varian Cary 5G spectrophotometer on a thin film of polymer deposited on a glass substrate to characterize the polymer conjugation length.

X-ray diffraction measurements were done in a  $\theta/2\theta$  Bragg–Brentano geometry by reflection with Cu  $K\alpha_1$  and  $K\alpha_2$  on a Siemens D5000 setup.

EDX measurements were carried out with a scanning electron microscope, JEOL 5800, at 7 keV.

Raman scattering measurements were done with a Jobin-Yvon T64000 at a laser excitation wavelength of 676.4 nm.

TEM characterizations were performed with an FEG Hitachi 2000 microscope.

## Results and Discussion

Porous silicon and silica matrixes were first characterized by different techniques.

To make sure that the pore orientation was essentially perpendicular to the silicon wafer surface, scanning electron microscopy was used on a cleaved sample. As a matter of fact, Figure 1 shows that during the anodization process the pores developed downward from the Si wafer surface with their axis perpendicular to the surface. The porous layer thickness was directly monitored by the reaction time at a given current density.

In Figure 2, it can be seen from this transmission electron micrograph that the pore walls are somewhat tortuous, showing sort of necks located at different places along the pores. An electron scattering experiment carried out on these features showed that one is dealing with silicon nanocrystals remaining in the walls. As seen from the above figures the pore diameter ranged between 50 and 15 nm at the neck location.

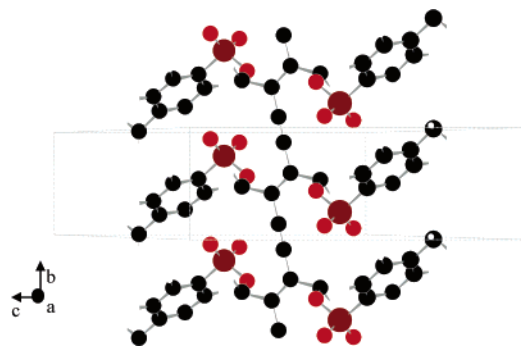


Figure 3. 100 projection of a single crystal of PTS showing the macromolecular chains along the  $b$  axis.

Table 1. BET Measurements on a Porous Silicon Layer (80% Porosity) before and after Its Thermal Oxidation

	specific surface area ( $\text{m}^2\cdot\text{g}^{-1}$ )	porous vol ( $\text{cm}^3\cdot\text{g}^{-1}$ )	av pore diam (nm)
porous silicon	323	1.64	18.8
porous silica	205	0.79	14.8

These values were corroborated by BET adsorption measurements,<sup>12</sup> which allowed us to get a mean value of the pore diameter either in porous silicon or in porous silica. The results are gathered in Table 1. It is to be noted that the mean diameter value obtained by this method was always lower than those observed by SEM (Figure 1). This difference comes probably from the pore tortuosity (Figure 2), and the diameter value given by this method is thus averaged, taking into account the existence of necks along the pores.

The monomer molecule dimensions (roughly 1.5–2 nm in its longest dimension) range well below the pore diameter values even at the pore necks. Therefore, monomers are able to penetrate without trouble into porous silica layers and can then crystallize when acetone is removed. However, several crystal orientations are possible: do monomer molecules lie with their two triple bonds parallel to the pore axis, that is, on the pore walls, or parallel to the pore bottom? Polymerization of DA–TS in the solid state occurs with a C–C bond tilt to build new covalent bonds between the monomers; it is thus essential to probe the polymer chain orientation.

Raman scattering has proved for a long time to be a powerful technique sensitive to polarizable electrons, as in conducting polymers.<sup>2</sup> Modes polarized along the PDA–TS chains may be chosen to probe chain orientation with polarized laser excitation.

The scheme in Figure 3 shows that polymer chains are aligned along the  $b$  axis of the PDA–TS monoclinic unit cell.<sup>11</sup> Interestingly, parallel lines were clearly visible on single-crystal faces: they correspond to the  $b$  axis, that is, to the PDA–TS chain axis, as evidenced by experimental X-ray diffraction.

Single crystals of PDA–TS were studied by Raman spectroscopy and X-ray diffraction in the same orientation by using a goniometer. The excitation wavelength used was 676.4 nm at 10 mW first with a nonpolarized light. We have obtained the well-known spectrum of PDA–TS, shown in Figure 4, in which interesting bands are located at  $952\text{ cm}^{-1}$

(12) Brunauer, S.; Emmett, P. H.; Teller, E. *J. Am. Chem. Soc.* **1938**, *60*, 309.

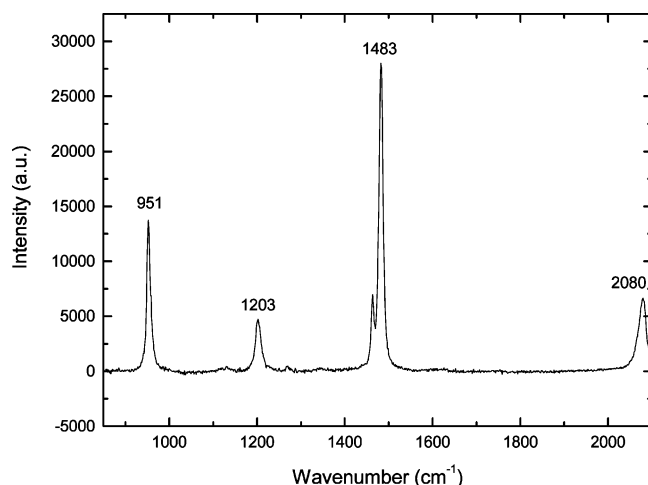


**Figure 4.** Nonpolarized Raman spectrum of a cleaved side of a nano-composite PDA-TS-porous silica in the middle of the layer ( $\lambda = 676.4$  nm).

(C—C stretching),  $1203\text{ cm}^{-1}$  (C=C bond scissor),  $1482\text{ cm}^{-1}$  (C=C), and  $2086\text{ cm}^{-1}$  (C≡C bond),<sup>14</sup> corresponding to the polymer backbone. X-ray diffraction data on this sample show a preferential 100 orientation of the surface, which means that the polymer chains are lying with this orientation (Figure 3). Furthermore, it has been known for some time that the band position corresponding to the C—C double bond is affected by the conjugation length.<sup>14</sup> In this sample the band was located at  $1482\text{ cm}^{-1}$  corresponding to a medium conjugation length, a so-called “purple phase”.<sup>14</sup>

The single crystal was further studied by polarized Raman scattering, which enables us to check the polymer chain orientation. In a micro Raman backscattering experiment, the excitation field and the backscattered one are in the same plane. By using one polarization parallel between the two fields (direction  $d$ ) and by turning around the same point with an amplitude of  $240^\circ$ , we see a maximum of intensity for the main bands ( $952$ ,  $1203$ ,  $1482$ , and  $2086\text{ cm}^{-1}$ ) corresponding to the polarization where the axis ( $d$ ) is oriented parallel to the polymer chains. So the intensity was fitted with eq 1 depending on the angle ( $\theta$ ) (angle between

$$I \propto [P_{aa} \cos(\theta) + P_{bb} \sin(\theta) + 2P_{ab} \sin(\theta) \cos(\theta)]^2 \quad (1)$$

the polymer chain orientation (axis  $b$ ) and the direction ( $d$ )). Assuming that the excitation beam is propagating along the  $c$  axis, the intensity of the scattered field for parallel polarized configurations can be written, in terms of the crystal polarizability tensor components  $P_{ab}$ , as a function of the angle  $\theta$  by eq 1.<sup>15</sup>

The fit shown as a dotted line presents a good correlation with experimental data for the PDA-TS single crystal with a  $\theta$  angle of  $180^\circ$  (or  $0^\circ$ ) at the maximum intensity that corresponds to the polymer chain and the polarized light collinear as shown in Figure 5.

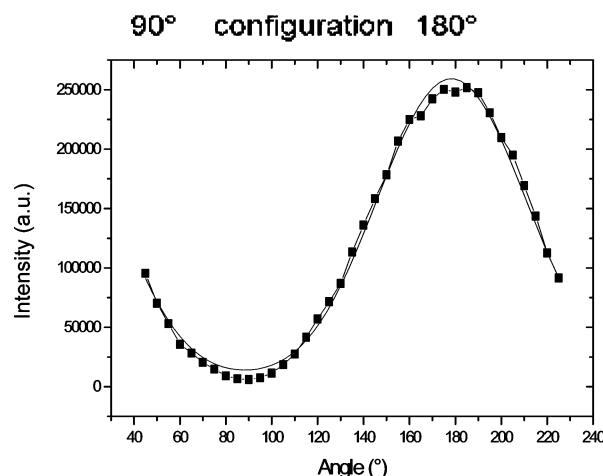
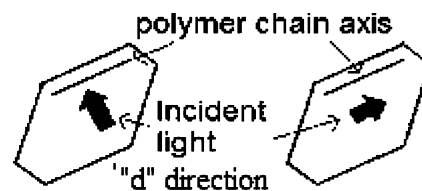


**Figure 5.** Intensity evolution of the  $1482\text{ cm}^{-1}$  band as a function of the angle ( $\theta$ ) measured by polarized Raman scattering spectroscopy ( $\lambda = 676.4$  nm).

The PDA-TS filling factor in the matrix was estimated by two methods.

The first estimation of the porous layer filling factor was obtained with EDX experiments in the scanning electron microscope. This technique was used either on a porous silica monolayer or on a bilayer with the S content as a probe of the polymer concentration.<sup>16</sup>

The second one was Raman scattering. These two methods show that the polymer is homogeneously embedded in the porous silica monolayer (Figure 6a). The atomic sulfur content has been measured to be 1.2% in this layer. It corresponds to a filling factor (calculated from the porosity) of 20% of the porous silica layer. The same work was done on porous silica bilayers. Measurements show that filling is not as homogeneous as in the case of a monolayer (Figure 6b). We can observe a concentration gradient from the top to the bottom of the pores. It seems that a kind of barrier exists at the interface of the two layers with different porosities. The atomic sulfur content ranges between 3.3% (filling factor 65%) in the upper layer and 2.2% (filling factor 40%) in the lower porous layer.

We were also able to measure the orientation of the polymer chains inside the pores (both on mono- and bilayers) with a polarized Raman scattering experiment, as explained previously in the case of a single crystal shown in Figure 5. The maximum corresponds to a polarization angle between  $80^\circ$  and  $100^\circ$  as seen in Figure 7. Therefore, we can conclude that the polymer chain axis is oriented following the pore axis. Such orientations have already been observed in other composites of mesoporous silica and conjugated polymers<sup>17,18</sup> made by the sol-gel process.

(13) Batchelder, D. N.; Bloor, D. *Advanced in infrared and Raman Spectroscopy*; Heyden-Wiley: Chichester, U.K., 1984; Vol. 11.

(14) Menzel, H.; Mowery, M. D.; Cai, M.; Evans, C. E. *J. Phys. Chem. B* **1998**, *102*, 9550.

(15) Congeduti, A.; Nardone, A.; Postorino, P. *Chem. Phys.* **2000**, *256*, 117.

(16) Errien, N.; Joubert, P.; Chaillou, A.; Mahric, C.; Godon, C.; Louarn, G.; Froyer, G. *Mater. Sci. Eng., B* **2003**, *100*, 259.

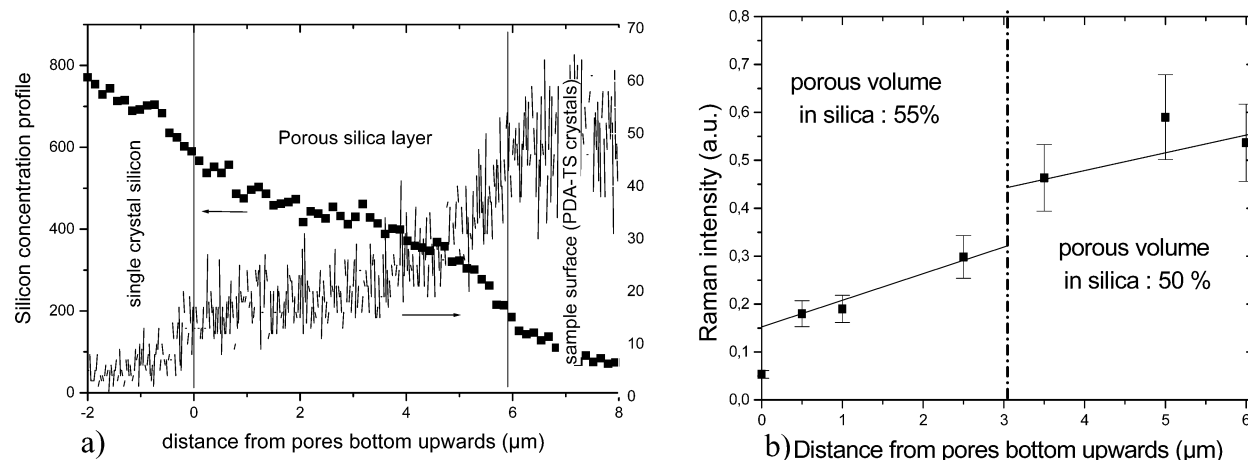
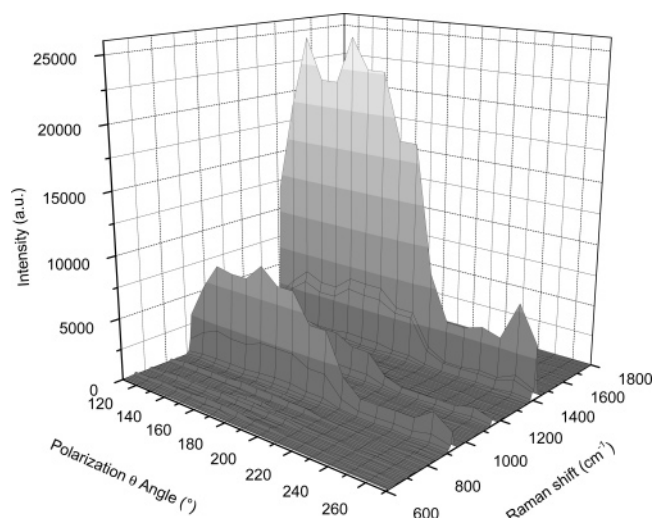
(17) Lin, V. S. Y.; Radu, D. R.; Han, M. K. *J. Am. Chem. Soc.* **2002**, *124*, 9040.



**Table 2. Orientation Factor of the Polymer Chains Inside Pores As Estimated by the Ratio  $I_{\max}/I_{\min}$  versus the Filling Factor Obtained from the Sulfur Content<sup>a</sup>**

	single crystal	upper porous silica layer	lower porous silica layer	low-porosity monolayer
filling factor as determined by EDX (estimated from the S content)				
ratio $I_{\max}/I_{\min}$ of the 1482 $\text{cm}^{-1}$ band	100	high (65%) 40	medium (40%) 20	low (10%) 12

<sup>a</sup> The orientation factor is normalized at 100 for a single crystal.

**Figure 6.** Concentration profiles of the PDA-TS inside (a) a monolayer of porous silica as obtained by EDX spectroscopy and (b) a bilayer as obtained by Raman scattering spectroscopy ( $\lambda = 676.4 \text{ nm}$ ,  $1482 \text{ cm}^{-1}$  band).**Figure 7.** Intensity evolution of the PDA-TS Raman spectrum as a function of the orientation of the polarized light inside a monolayer of porous silica as obtained by polarized Raman scattering ( $\lambda = 676.4 \text{ nm}$ ).

If we compare the ratio  $I_{\max}/I_{\min}$  as shown in Table 2, we observe that the higher the filling factor with PDA-TS (as measured by EDX), the higher the  $I_{\max}/I_{\min}$  ratio. This seems to indicate that the best orientation was obtained when the pores were fully occupied by the polymer. The PDA-TS chain orientation is induced by the monomer crystallization as mentioned before, but the way the molecules organize themselves on the pore surface is the key point which remains to be explained.

The same orientation effect was obtained in a porous silicon matrix as measured by polarized Raman scattering. As the surface energy of silica is quite different from that of silicon, even slightly oxidized as is the porous silicon used in our experiments (N. Errien, thesis), it is not clear whether this orientation phenomenon is due to a confinement effect or a surface effect. Further investigations are under way to clarify this point.

The nonlinear optical properties of the nanocomposite (monolayer) were examined by the I-scan technique,<sup>19</sup> showing an  $n_2$  value (third-order nonlinear refractive index of  $4 \times 10^{-15} \text{ m}^2 \cdot \text{W}^{-1}$ ) ranging at least 1 order of magnitude higher than that of the bulk polymer material. Since the guiding properties seem to be promising,<sup>20</sup> this improved composite should present interest in the telecommunication component for all optical signal processing.

## Conclusion

We have demonstrated that it is possible to obtain a new nanocomposite material by embedding uniformly conjugated polymers into a porous silica matrix. This method allows a homogeneous layer of hybrid material with promising large optical nonlinearity to be obtained. We have also detected the orientation of polymer chains of PDA-TS along the pore axis, pointing out a possible confinement effect which remains to be elucidated.

**Acknowledgment.** We acknowledge the financial support of the “Bretagne” and “Pays de Loire” regions, through Project PRIR, and D. Eon and V. Raballand (LPCM) for their technical help.

CM0500657

(18) Schwartz, B. J.; Nguyen, T. Q.; Wu, J. J.; et al. *Synth. Met.* **2001**, *116*, 35.

(19) Skarka, V.; et al. O-33 PSST, Valencia, Spain, 2004.

(20) Pirasteh, P.; et al. P2-84 PSST, Valencia, Spain, 2004.